Results in Physics 7 (2017) 2213–2223

Contents lists available at ScienceDirect

Results in Physics

journal homepage: www.journals.elsevier.com/results-in-physics

Disclosing the structural, phase transition, elastic and thermodynamic properties of $CdSe_{1-x}Te_x$(x = 0.0, 0.25, 0.5, 0.75, 1.0) using LDA exchange correlation

M. Jamal [a,*], M.S. Abu-Jafar [b,*], Diana Dahliah [b]

[a] Young Researchers and Elite Club, Islamshahr Branch, Islamic Azad University, Tehran, Iran
[b] Physics Department, An-Najah N. University, P.O. Box 7, Nablus, Palestine

ARTICLE INFO

Article history:
Received 30 March 2017
Received in revised form 20 June 2017
Accepted 21 June 2017
Available online 28 June 2017

Keywords:
Phase transition
Elastic properties
Thermodynamic properties
ZB and WZ

ABSTRACT

The phase transition and structural, elastic, thermodynamic characteristics of $CdSe_{1-x}Te_x$ alloys for all compositions x (x = 0, 0.25, 0.5, 0.75, 1) in both hexagonal wurtzite (WZ) and cubic zinc-blende (ZB) are studied at zero K and zero pressure in emphasis of the Full Potential Linearized Augmented Plane Wave (FP-LAPW) approach, in accordance with the Density Functional Theory (DFT). This was inserted within the WIEN2k code, alongside a local density approximation (LDA) in order to consider the exchange-correlation functional. For all compositions the $CdSe_{1-x}Te_x$ alloys were found to be mechanically stable for both phases ZB and WZ, and the strongest material among all structures is CdSe. Our findings reveal that the relation between elastic constants and the Te concentrations is not linear. The induced phase transition from ZB to WZ is studied at zero K, and the corresponding volume collapses at the phase transition boundary are calculated for all compositions x (x = 0.0, 0.25, 0.50, 0.75). Our results show that for all compositions of the $CdSe_{1-x}Te_x$ alloys, the stable phase is zinc-blende. Furthermore, the elastic characteristics of ZB and WZ phases of $CdSe_{1-x}Te_x$ alloys, alongside elastic constants, bulk modulus and shear modulus were determined and assessed in comparison with other theoretical and experimental findings available. A positive relationship was observed.

Introduction

Cadmium-Selenide-Telluride ternary alloys ($CdSe_{1-x}Te_x$) have a prominent place in modern semiconductor physics and devices technology due to the high absorption coefficient and the direct band gap corresponding to a wide spectrum of the wavelength from ultra-violet to infra-red regions [1,2,3], where the band gap of CdTe films are found to have a range from 1.49 to 1.53 eV and for CdSe from 1.9 to 1.7 eV [4]. The band gap of the ternary $CdSe_{1-x}Te_x$ lies between these two values, which can be tuned by varying the molar composition on the thickness of the film [4]. The broad and tunable absorption and emission wavelength ranges, and remarkable semiconducting properties of $CdSe_{1-x}Te_x$ alloys make them a good candidate for conversion of solar energy into photovoltaic or photo electrochemical devices [5,6]. Additionally, $CdSe_{1-x}Te_x$ alloys find extensive applications in photo electrochemical solar cells [7–10], transistors, photoconductors [11], solar control applications [10], and photo assisted decomposition of water [2].

The knowledge of the physical and fundamental properties of $CdSe_{1-x}Te_x$ will help in sampling, designing, and fabricating the technological devices in an effective way. The structural phase of ternary $CdSe_{1-x}Te_x$ depends on its molar composition, since the CdTe crystallized in the cubic form, while CdS and CdSe are most stable in form of hexagonal wurtzite[12], while the experimental results showed that $CdSe_{1-x}Te_x$ can be crystallized in either cubic or hexagonal structures [13–17]. Schenk and Silber [13] studied the microhardness of $CdTe_{1-x}Se_x$ alloys, who discovered that the cubic phase occurs in the composition extent $0 < x_{CdSe} < 0.45$, and the hexagonal phase in the extent $0.65 < x_{CdSe} < 1.0$. On the other hand, Uthanna et al. [14], Mangalhara et al. [15] and Islam et al. [16] found that $CdSe_xTe_{1-x}(0 \leq x \leq 1)$ ternary thin films, independent of composition, are zinc-blende (cubic phase). The new work of Shinde et al. [17], using an X-ray diffraction study, revealed that $CdSe_{0.6}Te_{0.4}$ thin films exhibit a hexagonal crystal structure in nature. There have been fewer studies on $CdSe_{1-x}Te_x$ nanocrystals [18–20]. Their experimental results showed that the physical and photoelectrical properties depend on the preparation method,

* Corresponding authors.
E-mail addresses: m_jamal57@yahoo.com (M. Jamal), mabujafar@najah.edu (M.S. Abu-Jafar).

http://dx.doi.org/10.1016/j.rinp.2017.06.033
2211-3797/

deposition time, and the temperature [21–23]. The $CdSe_{1-x}Te_x$ formed in amorphous film for small thickness less than 200 nm, and for higher value of thickness films were found to be polycrystallized in nature of a hexagonal phase [24]. The band gap was found to be affected by the thickness of the film and the concentration of Te, where the energy band gap decreases by increasing the Te concentration and by increasing the film thickness. For example, Das [25] utilized $CdSe_{1-x}Te_x$ alloys in order to investigate the main needs of an appropriate thin film photo electrode for high efficiency photo electrochemical cells. Ravichandran et al. [26] fabricated $CdSe_{1-x}Te_x$ thin film with different Te concentrations using the electro-deposition technique; the photoconductivity of these films was studied at different light intensities, and wavelength, as an operation of the applied DC-electric field. They showed that when the Te concentration for $CdSe_{1-x}Te_x$ increases, the gap of the energy band shrinks. The bowing of the band gap and the transformation of the structural phase of hot wall deposit $CdSe_{1-x}Te_x$ thin films were studied by the Muthukumarasamy et al. [27] for different Te concentrations. They reported a band gap of 1.45 eV for $CdSe_{0.6}Te_{0.4}$ thin film, which is very close to the perfect band gap (1.4 eV) for a solar cell. The most recent works by Shinde et al. [17,28] investigated the structural, optical, and photoelectrochemical properties of $CdSe_{0.6}Te_{0.4}$ thin films using different methods.

The elastic constants and thermodynamic properties of $CdSe_{1-x}Te_x$ are calculated theoretically, with the use of optimum values of the structures which are extracted from the 2D-search of the equation of the state [29] for hexagonal phase of $CdSe_{1-x}Te_x$ and under the FP-LAPW method [30] based on the Density Functional Theory (DFT) [31] within LDA [32] exchange-correlation potential. Since LDA exchange-correlation depicts structural parameters of CdSe and CdTe [33] better than PBE-GGA [34], it is worth adding some fundamental properties for both hexagonal and cubic phases of $CdSe_{1-x}Te_x$ and for all compositions x (x = 0, 0.25, 0.5, 0.75, 1), especially given that there is no experimental data in the literature except on elastic constants of hexagonal CdSe and zinc-blende CdTe. Nevertheless there are some theoretical studies, which research the elastic constants of both CdTe and CdSe [33,35–37]. Lately, Jamal et al. [38] showed that, within the PBE-GGA exchange-correlation, zinc-blende and the wurtzite structures of $CdSe_{1-x}Te_x$ are mechanically stable through the aforementioned span of Te concentration (0, 0.25, 0.5, 0.75, 1). Also, their calculations showed that the concentrations of Te or Se correlate non-linearly with the elastic constants. The pseudopotential plane wave approach was used to investigate the elastic constants of ternary $CdSe_xTe_{1-x}$ alloys with Se concentration (0, 0.3, 0.5, 0.7, 1) within the LDA potential for cubic and hexagonal phases [33,37].

Thus, structural parameters and elastic constants, and as a consequence thermodynamic properties are studied using the LDA exchange-correlation potential, to give a better description of exchange-correlation functional [33] in order to provide reference data for experimenters. This will provide essential evidence regarding the binding characteristic between adjacent atomic planes and the anisotropic character of binding and structural stability. Also, the phase transition and stable phase of $CdSe_{1-x}Te_x$ within LDA exchange-correlation are investigated due to previously mentioned different results of experimental works on the stable phase of $CdSe_{1-x}Te_x$.

Computational details

The optimum parameters (volume, energy, bulk modulus and derivate of bulk modulus) and optimized c/a ratio, and as a consequence optimized an and c lattice parameters for hexagonal phase of $CdSe_{1-x}Te_x$, also phase transition, mechanical and thermodynamic characteristics were studied on the basis of First-principle computations by utilizing the 2DR-optimize package [39], Gibbs program [40] and the IRelast package [41] which come with the WIEN2k package [42]. The elastic constants were estimated by fitting the second derivative of the energy with respect to strain to polynomial fit using IRelast package. Also phase transition, mechanical and thermodynamic properties of hexagonal phase of $CdSe_{1-x}Te_x$ were studied using optimum parameters from 2D-search of EOS. 2D-search of EOS, the method of elastic constants calculations and linked properties for wurtzite (hexagonal) and zinc-blende (cubic) symmetries are described in our earlier publications in more detail [29,43,44].

Our original method to estimate pressure-induced phase transition is to compute difference of Gibbs-free-energy for both phases of ternary $CdSe_{1-x}Te_x$ at the same pressure grid and at zero-temperature. As we know, G = E + PV − TS at $T \neq 0$ and therefore at zero temperature (T = 0) it will be G = E + PV. The above equation indicates that we must compute the energy (E) and volume (V) at any pressure (*P*) for both WZ and ZB phases. To achieve this aim, at the first step we find Murnaghan's equation of state (see following equation) using the calculated total energy as a function of volume (volume and c/a) changes for ZB (WZ) phase, which we can call '1D-search (2D-search) of EOS for ZB (WZ) phase'.

$$E(V) = E_0 + \frac{BV}{B'}\left\{1 + \frac{1}{B'-1}\left(\frac{V_0}{V}\right)^{B'}\right\} - \frac{BV_0}{B'-1}$$

The calculation of optimized parameters (E_0 – optimize denergy, V_0 – optimized volume, B – bulk modulus, B′ – derivative of bulk modulus) using Murnaghan's equation of state makes us able to find the volume and energy at any pressure, and as a consequence the Gibbs-free-energy is accessible.

$$V(P) = V_0\left\{1 + P\left(\frac{B'}{B}\right)\right\}^{\frac{-1}{B'}}$$

$$E(P) = E_0 + \frac{BV(p)}{B'}\left\{1 + \frac{1}{B'-1}\left(\frac{V_0}{V(p)}\right)^{B'}\right\} - \frac{BV_0}{B'-1}$$

Now, the above equations are used to evaluate the difference of Gibbs-free-energy (ΔG) for both phases on the same pressure grid.

The calculations have been performed in the framework of the DFT [31], and we have employed the FP-LAPW method [30], as implemented in the WIEN2k code [42]. We have used the LDA for the calculation of exchange-correlation energy functional [32], which is the recommended exchange-correlation functional for our compounds [33]. The wave functions were expanded with a cut off of $R_{MT} \times K_{max} = 9$ in the interstitial region, while in the muffin tin spheres they expanded, in the form of spherical-harmonics, up to $l_{max} = 10$ while the charge density was Fourier expanded up to $G_{max} = 12$. In the full Brillouin zone, k-point numbers were 2000 and 3000 k-points in the phases of wurtzite and zinc-blende.

The atoms' location was displaced, due to the internal coordinates during the process of elastic constants and the 2D-search computations, until the forces go around (1 mRy/bohr).

Results and discussion

-Structural properties

The optimal parameters of the lattice for $CdSe_{1-x}Te_x$ ternary alloys in different concentrations (x = 0, 0.25, 0.5, 0.75, 1), in the ZB and WZ phases, are computed to be utilized in the elastic constants (ECs) of interested compounds at zero pressure. 2D-search of EOS (volume and c/a structure optimization) using the 2DR-optimize package [39] is used to find the EOS for the hexagonal

Table 1
The structural parameters of the zinc-blende and wurtzite phases of $CdSe_{1-x}Te_x$ (x = 0.0, 0.25, 0.5, 0.75, 1.0) alloys compared with theoretical and experimental data.

Compounds	a (Å)	c (Å)	B (GPa)	B′
$CdSe_{cubic}$	6.019		58.89	4.85
Theor	6.207,[a]6.210,[b]6.050[c]		45.60[a],65.12[c]	
Exp	6.052,[f]6.084,[g,h]6.050[j]		53.00[i]	
$CdSe_{wurtzite(2D)}$	4.250	6.950	57.19	4.59
Theor	4.340,[a]4.270[j]	7.270,[a]6.980[j]	43.64[a]	
Exp	4.300[l]	7.010[l]		
$CdSe_{0.75}Te_{0.25\ cubic}$	6.121		55.29	4.88
Theor	6.526[a]		43.08[a]	
$CdSe_{0.75}Te_{0.25\ wurtzite(2D)}$	4.323	14.142	54.21	4.78
Theor	4.429[a]	14.891[a]	42.32[a]	
$CdSe_{0.5}Te_{0.5\ cubic}$	6.220		52.05	4.89
Theor	6.407[a]		42.21[a]	
$CdSe_{0.5}Te_{0.5\ wurtzite(2D)}$	4.392	7.196	50.84	4.78
Theor	4.437[a]	7.459[a]	39.14[a]	
$CdSe_{0.25}Te_{0.75\ cubic}$	6.319		49.16	4.90
Theor	6.322[a]		40.14[a]	
$CdSe_{0.25}Te_{0.75wurtzite(2D)}$	4.462	14.619	48.13	4.80
Theor	4.563[a]	14.653[a]	36.31[a]	
$CdTe_{cubic}$	6.415		46.59	4.91
Theor	6.620,[a]6.626,[b]6.480,[c]6.540[m]		36.24,[a]48.94[c]	
Exp	6.480,[f]6.540,[h]6.477[m]		44.50[i]	
$CdTe_{wurtzite(2D)}$	4.529	7.438	46.34	4.91
Theor	4.680,[a]4.560,[m]4.480[j]	7.650,[a]7.540,[m]7.360[j]	34.62[a]	
Exp	4.570[m]	7.470[m]		

[a] Ref. [50].
[b] Ref. [45].
[c] Ref. [35].
[f] Ref. [45].
[g] Ref. [46].
[h] Ref. [47].
[i] Ref. [48].
[j] Ref. [33].
[l] Ref. [51].
[m] Ref. [49].

phase since the equation of state has two degrees of freedom such as volume and c/a. Our prior works show that a two-dimensional search of EOS can be necessary [43,29] and displays the exactness of the method of calculations (DFT in this case) better than a one-dimensional search (i.e. volume changes) of EOS.

Our results are listed and compared in Table 1, along with theoretical results and experimental data. For zinc-blende (cubic) symmetry of CdSe (x = 0) and CdTe (x = 1), our calculated **a**-lattice constant using LDA is underestimated when compared with the experimental data [45–49] and earlier DFT-LDA computations [35], and is in very good accordance with the experimental reports. However, it can be clearly seen that our results are in excellent agreement with the previous [35] DFT-LDA calculation. For x = 0.25, x = 0.5 and x = 0.75 our LDA **a**-lattice parameters are smaller than those conveyed by Reshak et al. [50]. Although we used the same package (WIEN2k) and therefore the same approach (FP-LAPW), our number of k-mesh points we used in the full Brillouin zone were 3000 so we selected $l_{max} = 10$ with different exchange-correlation (LDA), whilst they used 1400 k-points and $l_{max} = 6$ with PBE-GGA exchange-correlation in their calculations [50]. This is potentially the main explanation for the disagreement in results.

Table 1 shows the structural parameters data for both ZB and WZ phases. As the Te concentration increases, the lattice parameter for ZB $CdSe_{1-x}Te_x$ within LDA exchange-correlation increases monotonically. On the other hand, the bulk modulus decreases monotonically.

The same behavior can be seen in derivatives of bulk modulus with a monotonic variation. However, the variation for derivatives of bulk modulus with increasing Te concentration is so small. For hexagonal (wurtzite) CdSe (x = 0) *and* CdTe (x = 1), our computed *a* and *c* lattice constants within LDA are underestimated with respect to the experimental data [49,51]. However, one can see that our results confirm the previous DFT-LDA calculations [33]. For x = 0.25, x = 0.50 and x = 0.75, our LDA lattice parameters **a** and **c** are a little bit smaller than that conveyed by Reshak et al. [50]. However, the lack of agreement originates from the different k-points, the value of l_{max} and the exchange-correlation functional utilized in past and present calculations.

Our results show that as the concentrations of Te changes from zero to one in the hexagonal symmetry, the lattice constant **a** increases monotonically. At the same time, the bulk modulus decreases monotonically within LDA potential when shifting from wurtzite-CdSe to wurtzite-CdTe, as seen in Table 1.

As can be seen in Table 1 for hexagonal phase, approximately the derivative of bulk modulus is increasing as the Te concentration increases. Nevertheless, the variation is so small as we shift from wurtzite-CdSe to wurtzite-CdTe. As the bulk modulus means that there is a resistance against the volume changes, it is clear that decreasing Se concentration (increasing the Te value) in ternary $CdSe_{1-x}Te_x$ alloys leads to the reduction in hardness (resistance to changes in volume) for both phases. Our results show that increasing the Te content leads to decreasing energy at about −1091.05 and −1091.03 (Ryd/atom) for cubic and wurtzite phases as we shift from CdSe to CdTe, respectively. This means that we expect to see a linear equation when we fit the optimized energy based on the Te content.

In order to find the effect of increasing the Te content regarding the **a**-lattice constant, the bulk modulus and the optimized energy of ternary $CdSe_{1-x}Te_x$ alloys within LDA potential for both cubic and hexagonal phases and prediction analytical expressions for them, we have obtained the following polynomial fit (order of fit 2):

$$a_C(x) = -0.014x^2 + 0.410x + 6.019$$
$$a_H(x) = -0.013x^2 + 0.291x + 4.250$$
$$B_C(x) = 2.754x^2 - 15.0463x + 58.886$$
$$B_H(x) = 3.474x^2 - 14.586x + 57.332$$
$$E_C(x) = -0.004x^2 - 4364.192x - 8018.133$$
$$E_H(x) = 0.055x^2 - 4364.201x - 8018.125$$

Where a shows the **a**-lattice constant for hexagonal (H) and cubic (C) phases in units of angstrom, B represents the resistance against the volume changes (bulk modulus) in units of (GPa) and E exhibits optimized energy in units of (Ryd/atom).

As can be seen from the above equations, the **a**-lattice constants for the cubic and wurtzite phases have swerved slightly from the linearity as a function of Te concentration (x). The above equations show that the deviation from linearity regarding the **a**-lattice parameter for the cubic phase is bigger than that of the wurtzite phase. Our fitting indicates that bowing parameters of bulk modulus is larger than the **a**-lattice parameter, which confirms the non-linear behavior of bulk modulus against x changes as long as the bowing parameter of the hexagonal phase from linearity is larger than that of the ZB phase. Our fitting regarding the optimized energy indicates that the optimized energy of the ZB phase has swerved slightly from linearity as function of x changes, however the divergence from linearity in the WZ structure is larger than that in the ZB structure.

Elastic constants

The IRelast package [41] is used to calculate the elastic constants of ZB and WZ phases of $CdSe_{1-x}Te_x$ alloys at zero-temperature and zero-pressure and at various Te composition (x = 0.0, 0.25, 0.5, 0.75, 1.0) at their optimized lattice parameters. Tables 2 and 3 show these values along with experimental data [52,53] and earlier theoretical calculations [33,36,37]. Theoretical calculations of the ECs guide us to give estimation for the important technological characteristics such as hardness, brittleness/-ductility, stiffness, and types of bonds for our substance of interest.

The elastic constants help to predict the properties of the material such as the ductility of the material, which is determined by the value of the ratio of bulk modulus to shear modulus (B/S). If it is less than 1.75 [43] a material is treated as brittle, otherwise it is a ductile material. The type of bond in the structure can be determined by the indication of Cauchy pressure ($C_{12} - C_{44}$) (for hexagonal compound $C_{44} = C_{55}$). Generally, the Cauchy pressure of compounds with more prevailing ionic (covalent) bonds is positive (negative) [43], or by Poisson's ratio, for which the value is much less than 0.25 (around 0.1) for a typical covalent compound, and around 0.25 or higher for an ionic compound [54]. Moreover, our previous studies suggested the usual value $\nu = 0.236$ for Poisson's proportion as a limit for specifying type of bonds [43].

Stiffness is specified through the resistance against forces of deformation. As the material becomes stiffer with the larger the amount of young modulus (Y), we believe that there is a correlation between Young's modulus, which defines the ratio of stress to strain, and the level of stiffness. Hardness is specified by how much our material can resist when changing shape. There are three representatives for this. The first one is bulk modulus, which means "the resistance to volume changes". The second one is shear modulus, which means "resistance against reversible deformations" and the third one is Vickers hardness as $H_V^{Chen} = 2(k^2S)^{0.585} - 3(k = \frac{S}{B}, S - \text{shear and } B - \text{bulk modulus})$ [55]. Therefore, we have found that shear modulus can predict hardness better than bulk modulus [43] because it is resistant to reversible deformations, whilst new research of Chen et al. [55] reports that Vickers hardness again shows hardness better than shear modulus. Using Chen's equation negative Vickers hardness is predicted for some ionic compounds such as our compounds of interest in this research. The possibility of negative Vickers hardness is removed with the new Tian's equation as $H_V^{Tian} = 0.92k^{1.137}S^{0.708}$ [56]. When hardness is >5 (GPa), both formulas are in accordance with experimental data, but overestimate it at low hardness side [56]. As we know the Voigt and Reuss approximation estimate the higher and lower boundaries of

Table 2
The calculated elastic constant (C_{ij} in GPa), Bulk modulus (B), Shear modulus (S) and Young's modulus (Y) in Voigt (V)–Reuss (R)–Hill (H) approximations (in GPa), Poisson's ratio (ν), transverse elastic wave velocity (V_t in m/s), longitudinal elastic wave velocity (V_l in m/s), average wave velocity (V_m in m/s), Debye temperature (Θ_D in K) and Vickers hardness base on the Chen and Tian equations (H_V in GPa) for zinc-blende $CdSe_{1-x}Te_x$ (x = 0.0, 0.25, 0.5, 0.75, 1.0) alloys in comparison with available experimental and theoretical data.

Cubic	CdSe	$CdSe_{0.75}Te_{0.25}$	$CdSe_{0.5}Te_{0.5}$	$CdSe_{0.25}Te_{0.75}$	CdTe
C_{11}	71.36,**67.81**,[a]**88.4**[b]	67.79	64.41,**59.17**[a]	61.50	59.51,**57.38**,[a](53.51)[c]
C_{12}	53.43,**50.12**,[a]**38.3**[b]	49.48	46.33,**42.04**[a]	43.33	41.02,**39.19**,[a](36.81)[c]
C_{44}	23.34,**22.89**,[a]**35.7**[b]	22.75	22.96,**20.95**[a]	21.48	21.34,**21.31**,[a](19.94)[c]
B_V	59.40	55.58	52.35	49.38	47.19
B_R	59.40	55.58	52.35	49.38	47.19
B_H	59.40	55.58	52.35	49.38	47.19
S_V	17.59	17.31	17.39	16.52	16.50
S_R	14.22	14.27	14.21	13.90	14.01
S_H	15.90	15.79	15.80	15.21	15.26
Y_V	48.03	47.04	46.98	44.60	44.34
Y_R	39.50	39.43	39.10	38.12	38.24
Y_H	43.80	43.27	43.07	41.38	41.31
ν_V	0.365	0.358	0.350	0.349	0.343
ν_R	0.389	0.381	0.375	0.371	0.364
ν_H	0.377	0.370	0.362	0.360	0.354
V_t	1651.64	1636.57	1629.39	1592.62	1589.38
V_l	3718.38	3605.63	3512.18	3408.36	3343.93
V_m	1863.83	1845.08	1835.14	1793.11	1787.94
Θ_D	184.39	179.48	175.67	168.96	165.96
H_V^{Chen}	−0.842	−0.695	−0.525	−0.521	−0.371
H_V^{Tian}	1.457	1.552	1.663	1.657	1.775

Theoretical results are bold while Experimental results are given in parenthesis.
[a] Ref. [37] (LDA).
[b] Ref. [36].
[c] Ref. [52] (at 25 C).

Table 3
The calculated elastic constant (C_{ij} in GPa), Bulk modulus (B), Shear modulus (S) and Young's modulus (Y) in Voigt (V)–Reuss (R)–Hill (H)approximations (in GPa), Poisson's ratio (ν), transverse elastic wave velocity (V_t in m/s), longitudinal elastic wave velocity (V_l in m/s), average wave velocity (V_m in m/s), Debye temperature (Θ_D in K) and Vickers hardness base on the Chen and Tian equations (H_V in GPa) for wurtzite $CdSe_{1-x}Te_x$(x = 0.0, 0.25, 0.5, 0.75, 1.0) alloys in comparison with available experimental and theoretical data.

HEX	CdSe	$CdSe_{0.75}Te_{0.25}$	$CdSe_{0.5}Te_{0.5}$	$CdSe_{0.25}Te_{0.75}$	CdTe
C_{11}	81.11,**78.88**,[a]**62.76**,[b](74.6)[c]	76.60	72.43,**70.94**,[a]**53.88**[b]	69.09	67.03,**68.93**,[a]**51.99**[b]
C_{12}	49.25,**48.81**,[a]**36.39**,[b](46.1)[c]	45.66	42.24,**41.72**,[a]**30.37**[b]	40.27	38.32,**38.09**,[a]27.99[b]
C_{13}	42.55,**41.48**,[a]**30.17**,[b](39.4)[c]	39.66	36.80,**34.60**,[a]**24.53**[b]	33.93	32.08,**30.82**,[a]**22.17**[b]
C_{33}	90.34,**89.48**,[a]**70.36**,[b](81.7)[c]	86.23	82.81,**83.21**,[a]**61.84**[b]	79.74	78.18,**81.10**,[a]**60.34**[b]
C_{55}	13.29,**13.51**,[a]**11.93**,[b](13.0)[c]	12.88	12.50,**12.83**,[a]**10.56**[b]	12.22	12.59,**13.17**,[a]**10.61**[b]
B_V	57.92,**56.45**,[a]**50.90**,[b](53.4)[c]	54.37	51.04,**49.42**,[a]**41.98**[b]	48.24	46.35,**46.36**,[a]**38.70**[b]
B_R	57.91,**56.45**,[a]**50.90**,[b](53.4)[c]	54.35	51.00,**49.42**,[a]**41.98**[b]	48.21	46.31,**46.36**,[a]**38.70**[b]
B_H	57.91,**56.45**,[a]**50.90**,[b](53.4)[c]	54.36	51.02,**49.42**,[a]**41.98**[b]	48.22	46.33,**46.36**,[a]**38.70**[b]
S_V	16.38	15.87	15.47	15.09	15.22
S_R	15.69	15.21	14.81	14.39	14.57
S_H	16.04	15.45	15.14	14.74	14.90
Y_V	44.91	43.40	42.16	40.99	41.17
Y_R	43.17	41.74	40.50	39.26	39.56
Y_H	44.04	42.57	41.33	40.13	40.37
ν_V	0.370	0.366	0.362	0.358	0.351
ν_R	0.375	0.372	0.367	0.364	0.357
ν_H	0.373	0.369	0.364	0.361	0.354
V_t	1657.70,**1598.05**[a]	1622.12	1593.78,**1606.77**[a]	1566.81	1571.32,**1651.97**[a]
V_l	3686.17,**3661.09**[a]	3565.37	3456.47,**3433.46**[a]	3362.42	3312.25,**3294.34**[a]
V_m	1869.67,**1862.93**[a]	1828.60	1795.55,**1808.91**[a]	1764.29	1767.80,**1795.78**[a]
Θ_D	185.03,**183.82**[a]	178.00	171.95,**172.87**[a]	166.30	164.04,**168.42**[a]
H_V^{Chen}	−0.74	−0.72	−0.63	−0.59	−0.42
H_V^{Tian}	1.524	1.529	1.583	1.606	1.715

Theoretical results are bold while Experimental results are given in parenthesis.
[a] Ref. [33] (LDA).
[b] Ref. [33] (PBE-GGA).
[c] Ref. [48] (at 300 K).

mechanical characteristics [43]. Therefore thermodynamic properties, for example average sound velocity (V_m) along with the transversal (V_t) and longitudinal (V_l) sound velocities and Debye temperature (θ_D) are assessed through the application of the Hill method that is a half-value of Voigt and Reuss equations.

Table 2 demonstrates that the LDA elastic constants, which we calculated for cubic phase of CdSe and CdTe, are in good agreement and bigger than earlier theoretical LDA computations, as calculated by Benyettou et al. [37]. The difference between Benyettou et al.'s calculations and ours stems from the fact that we used FP-LAPW while they used the pseudopotential plane wave method.

Our calculated LDA elastic constants, cubic CdSe, in comparison with previous computations of Hannachi et al. [36], display a big difference for C_{11}, C_{12} and C_{44}. Our C_{11} and C_{44} are smaller than their calculations, while our C_{12} is larger. This difference can be considered from this fact that we employed FP-LAPW, whereas they utilized the empirical pseudopotential method. In the cubic phase of CdTe, our evaluated LDA elastic constants are in accordance with experimental result [52]. Nonetheless, previous LDA calculations [37] are in better accordance than our LDA computations. We should emphasize that our theoretical and Benyettou et al.'s [37] calculations are at zero-temperature while the experimental data were at 298 K. For cubic $CdSe_{0.5}Te_{0.5}$, our estimated elastic constants within LDA are larger than and in correlation with the previous LDA computations [37].

The elastic constants for the zinc-blende $CdSe_{1-x}Te_x$(x = 0.25 and 0.75) within LDA are calculated for the first time, which made them a servant for upcoming theoretical and experimental work.

The dominant bond for CdSe and CdTe in the form of ZB is an ionic bond which is proved by the positive indication of Cauchy pressure (C_{12}–C_{44} > 0) within LDA potential, which is the same as the sign of Cauchy pressure utilizing both experimental and theoretical elastic constants and also by our evaluated Poisson's ratio, in which we find them as ν = 0.377 and ν = 0.354 for cubic CdSe and CdTe, respectively (check Table 2). This means that for the second time, by using Poisson's ratio, we could estimate that cubic CdTe and CdSe are substances with ionic bonds. This is compatible with our estimation by applying the Cauchy pressure's sign. Our $\left(\frac{B_H}{S_H}\right)$ ratio for cubic CdSe and CdTe are 3.74 and 3.09. Such a prediction shows how the cubic CdSe has larger ductile properties than the cubic phase of CdTe.

The value of bulk modulus and shear modulus for ZB CdSe is of a greater value, thereby showing how ZB CdTe is softer than CdSe whilst Vickers hardness (Hill's data was applied) illustrates how CdSe is softer than CdTe.

Young's modulus values predict that ZB CdSe is stiffer than ZB CdTe. As can be seen in Table 2, elastic constants of cubic CdSe are bigger than cubic CdTe. Thus, we can describe that from a mechanical viewpoint, CdSe is more strong than CdTe.

Our calculations (see Table 2) indicate that the mechanical in addition to the thermodynamic characteristics, namely C_{11}, C_{12}, approximately C_{44}, Bulk modulus, approximately Young's modulus, Poisson's ratio, Debye temperature, transverse and longitudinal elastic wave velocities and average wave velocity for cubic $CdSe_{1-x}Te_x$ within LDA potential reduce monotonically. However Chen's Vickers hardness grows monotonically with the growth of the Te (decreasing the Se) concentration. Table 2 shows that C_{44} is not so sensitive to changes of Te content.

Our Poisson's ratio and Cauchy pressure (C_{12}-C_{44}>0) show that the strength of the ionic bond decreases by increasing the Te concentration. Bulk modulus and Hill's shear modulus results estimate that ZB CdSe is the hardest substance in all compositions x (x = 0, 0.25, 0.5, 0.75, 1) which this study looks at. However, Vickers hardness (Hill's data was applied) suggests that ZB of CdTe is the hardest substance. Furthermore, our computed Young's modulus suggests that ZB of CdSe is the stiffest substance, for all values of x (x = 0, 0.25, 0.5, 0.75, 1). The largest values of elastic constants are related to ZB of CdSe for all variations of x (x = 0, 0.25, 0.5, 0.75, 1). This denotes that from a mechanical viewpoint, cubic CdSe

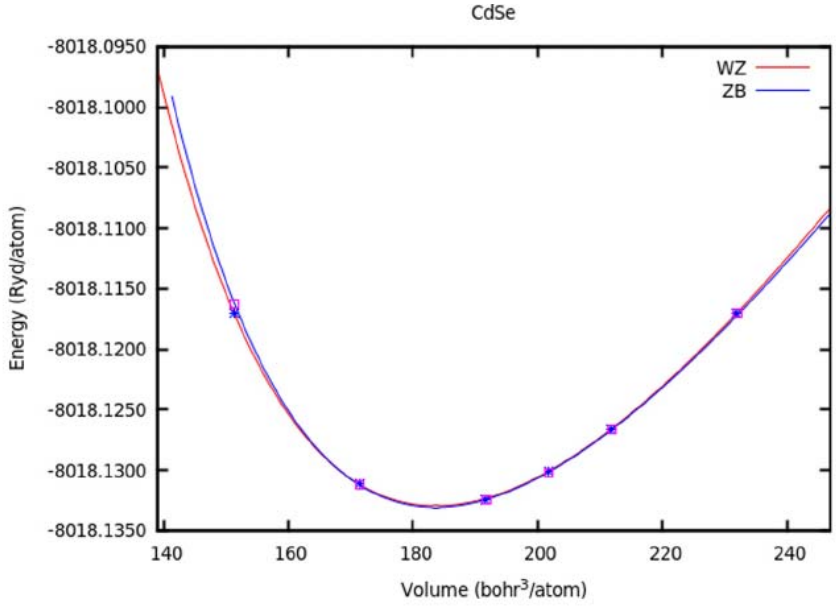

Fig. 1a. Equation of state for two phases of CdSe compound within LDA.

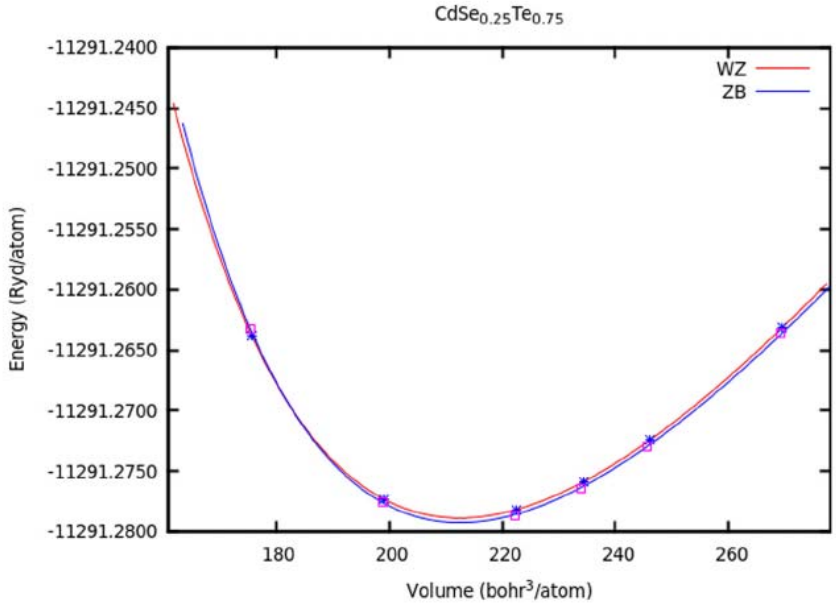

Fig. 1b. Equation of state for two phases of $CdSe_{0.25}Te_{0.75}$ compound within LDA.

is the strongest of all the substances of the cubic ternary $CdSe_{1-x}Te_x$ alloys (x = 0, 0.25, 0.5, 0.75, 1).

In order to find the effect of increasing Te content regarding the elastic constants of ZB ternary $CdSe_{1-x}Te_x$ alloys in LDA exchange-correlation and prediction analytical expressions for them, we have done the following polynomial fit as a function of Te concentration (order of fit 2):

$$C_{11}(x) = 4.149x^2 - 16.145x + 71.431$$
$$C_{12}(x) = 3.920x^2 - 16.308x + 53.402$$
$$C_{44}(x) = -0.903x^2 - 1.205x + 23.315$$

The above equations indicate that for C_{44} the bowing parameters are smaller than C_{11} and C_{12}, as the deviation from linearity for C_{11} is bigger than that of C_{12}. They present a non-linear relation between the elastic constants and Te concentration.

For cubic systems, the Born elastic stability conditions [57,58] are as following. It is clear that the third condition ($C_{11} > 0$) is an extra condition which is usually used because from the first two conditions we can derive the third one.

$$C_{11} - C_{12} > 0,\ C_{11} + 2C_{12} > 0,\ C_{11} > 0,\ C_{44} > 0$$

The above conditions (see Table 2) are evidently satisfied by our results. This shows that cubic ternary $CdSe_{1-x}Te_x$ alloys within LDA potential have a mechanical stability throughout the whole studied range (x = 0.0, 0.25, 0.50, 0.75, 1.0).

Our calculations of the elastic constants for hexagonal $CdSe_{1-x}Te_x$ ternary alloys within LDA potential are mustered in Table 3, along with experimental [53] and theoretical data [33]. To our knowledge, no simulated or experimental result exists for the elastic constants of hexagonal $CdSe_{1-x}Te_x$(x = 0.25 and 0.75) within LDA exchange-correlation. Our calculations are appending appro-

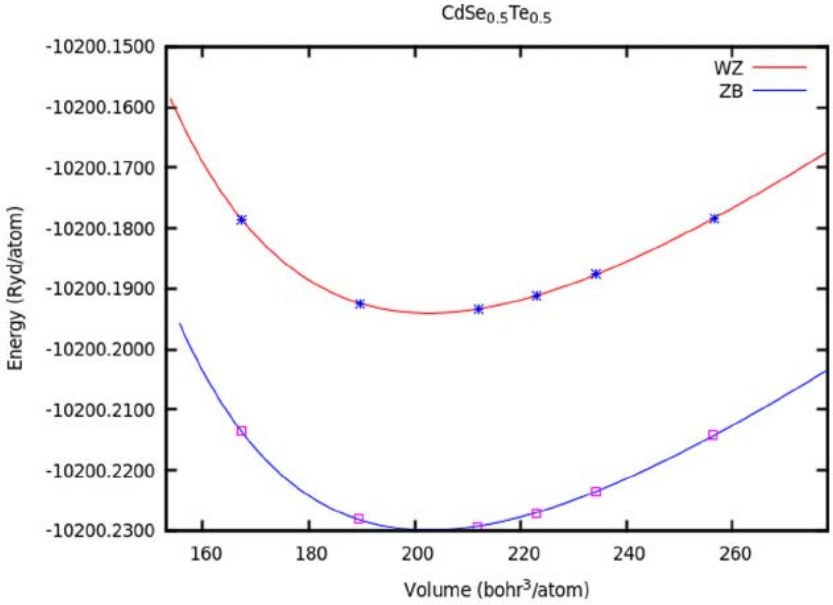

Fig. 1c. Equation of state for two phases of $CdSe_{0.5}Te_{0.5}$ compound within LDA.

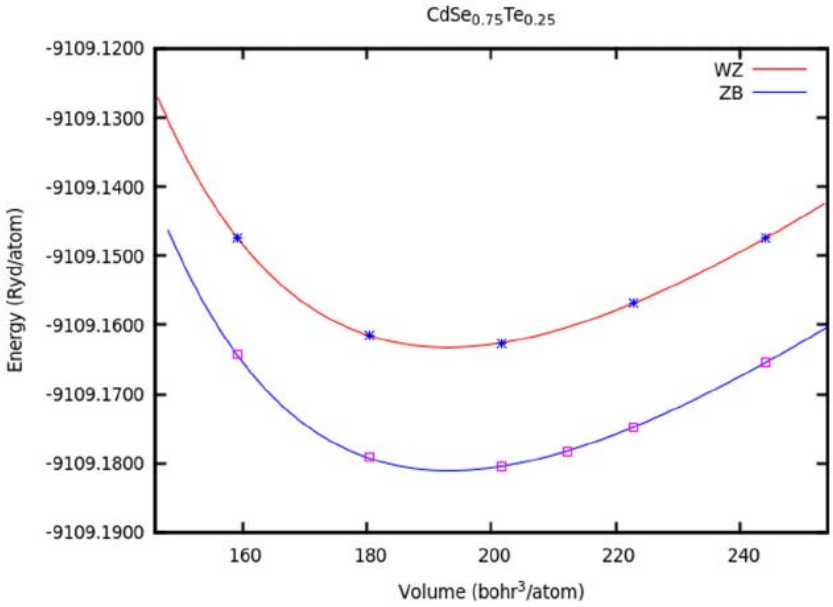

Fig. 1d. Equation of state for two phases of $CdSe_{0.75}Te_{0.25}$ compound within LDA.

priate data to this area of research, which we expect will provide a substantial source of information for future investigations.

Our findings show that our outcomes within LDA potentially agree very well with the earlier theoretical LDA computation [33] for x = 0.0, 0.50, 1.0 and the experimental result [53]. It is important to note that the evaluated elastic constants using LDA exchange-correlation are larger than earlier PBE-GGA computations produced by Saib et al. [33]. The lack of consistency between our results and the experimental results of hexagonal CdSe and CdTe is due to the fact that our simulated-data was carried out at zero temperature, whilst experiments were conducted at room temperature, as well as the absence of a precise choice of exchange-correlation functional. Also, as Table 3 indicates, the simulated data of CdSe presented by Saib et al. [33] using LDA potential are in further accordance with experimental results at 300 K, while for CdTe our results within LDA are in good accordance with the experimental results.

Our Poisson's ratio and Cauchy pressure (C_{12}–$C_{55} > 0$, for hexagonal symmetries $C_{44} = C_{55}$) within LDA exchange-correlation forecast that for hexagonal CdSe and CdTe compounds the dominant bonds are ionic bonds, and thus is in understanding with the sign of Cauchy pressure using experimental and theoretical elastic constants. Table 3 shows that Shear modulus and bulk modulus of hexagonal CdTe are smaller than hexagonal CdSe, which offers that CdSe is harder than CdTe, whilst Vickers hardness, evaluated using Hill's data, illustrates that hexagonal CdTe is harder than hexago-

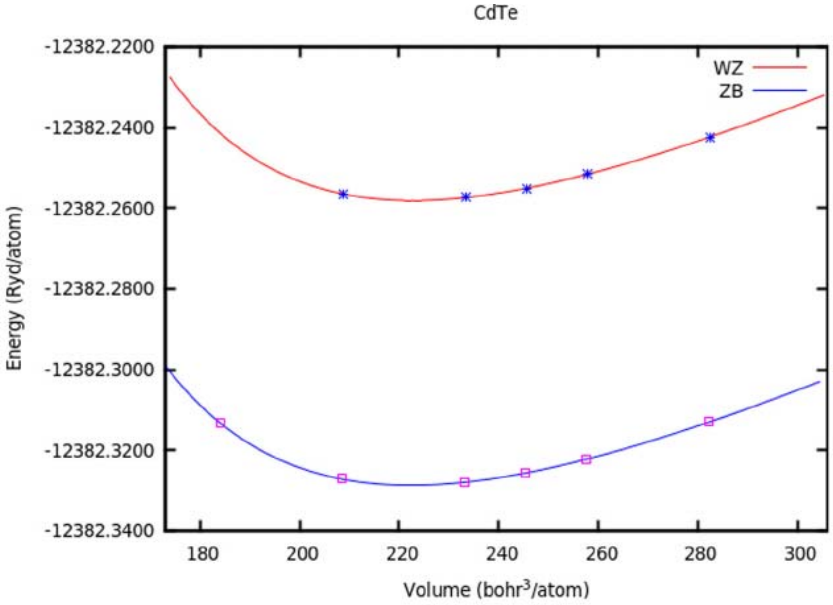

Fig. 1e. Equation of state for two phases of CdTe compound within LDA.

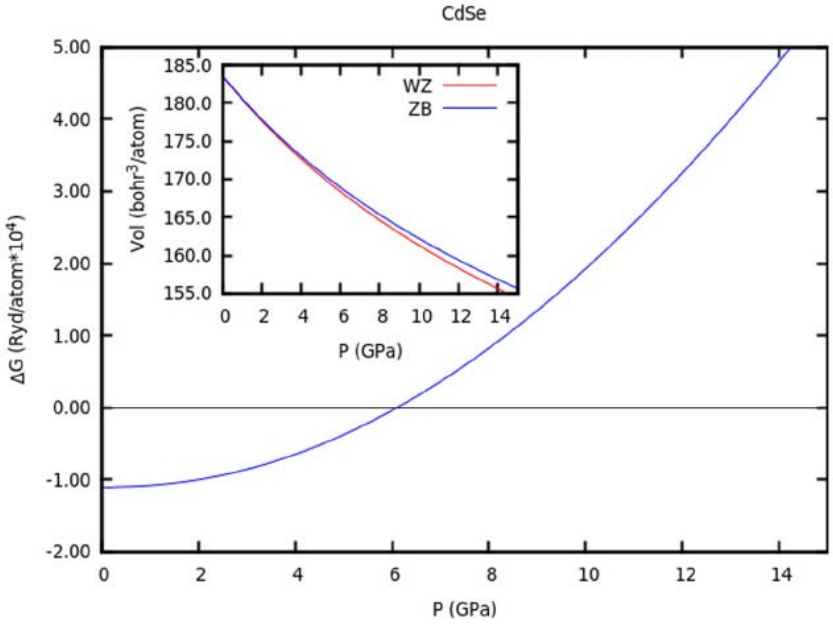

Fig. 2a. Difference of Gibbs free energy as function of pressure for two phases of CdSe compound within LDA. The inset: Calculation of the volume versus pressure for two phases.

nal CdSe. Compared to the hexagonal CdTe, Young's modulus of hexagonal CdSe is larger. This suggests that hexagonal CdSe is stiffer than hexagonal CdTe. The ratio of Hill's bulk modulus and Hill's shear modulus $\left(\frac{B_H}{S_H}\right)$ for hexagonal phase of CdSe and CdTe (3.61 and 3.11, respectively) estimates that hexagonal CdSe is more ductile than hexagonal CdTe.

Our simulated results show that the elastic constants of hexagonal CdTe are smaller than hexagonal CdSe. Therefore, from a mechanical viewpoint CdSe is stronger than CdTe, which is in alignment with the earlier theoretical estimation [33].

As Table 3 shows, the mechanical and thermodynamic characteristics, namely C_{11}, C_{12}, C_{13}, C_{33}, approximately C_{55}, approximately Bulk, Shear and Young's modulus, Poisson's ratio, longitudinal elastic wave velocity, approximately transverse elastic and average wave velocities and Debye temperature for hexagonal $CdSe_{1-x}Te_x$ within LDA potential are reduced monotonically with growth of Te content.

The value of Poisson's ratio and the value of Cauchy pressure (C_{12}–$C_{55} > 0$) suggest that for hexagonal $CdSe_{1-x}Te_x$ ternary alloys within LDA potential, dominant bonds are ionic bonds for all compositions x (x = 0.0, 0.25, 0.50, 0.75, 1.0) of interest.

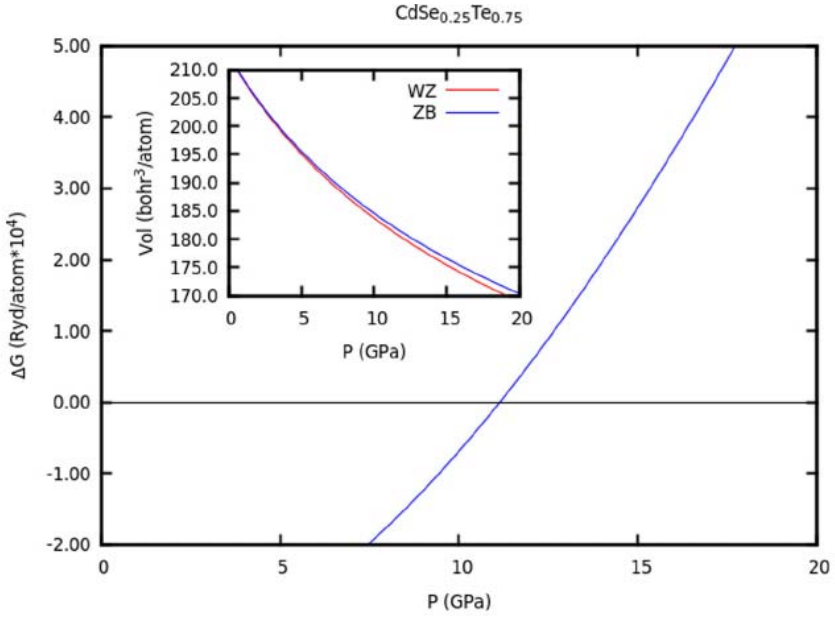

Fig. 2b. Difference of Gibbs free energy as function of pressure for two phases of $CdSe_{0.25}Te_{0.75}$ compound within LDA. The inset: Calculation of the volume versus pressure for two phases.

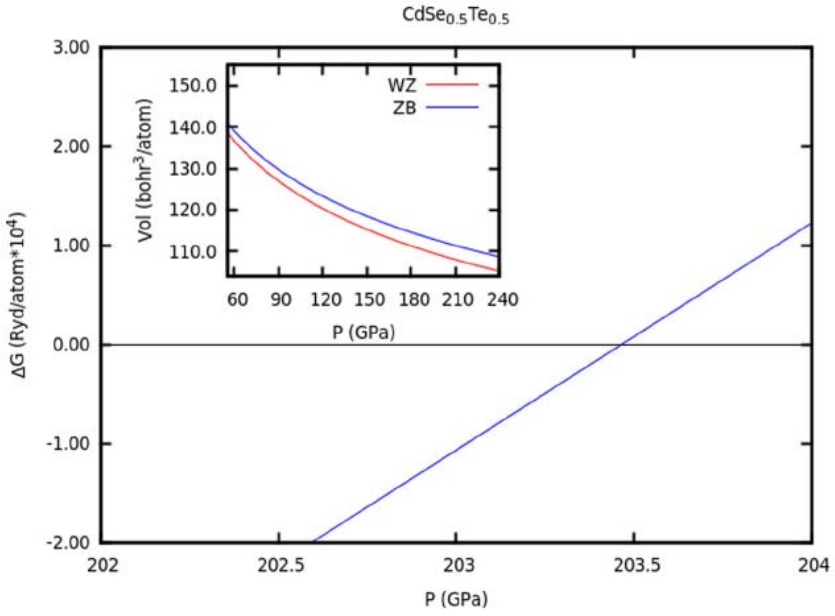

Fig. 2c. Difference of Gibbs free energy as function of pressure for two phases of $CdSe_{0.5}Te_{0.5}$ compound within LDA. The inset: Calculation of the volume versus pressure for two phases.

The computed bulk and shear modulus which we have calculated predicts that hexagonal *CdSe* is the hardest substance for all compositions x (x = 0.0, 0.25, 0.50, 0.75, 1.0) of relevance. But Vickers hardness (Hill's data was used) suggests hexagonal CdTe as the hardest substance.

The available data of Young's modulus (see Table 3) indicate that hexagonal CdSe can be understood as the stiffest substance for all variations of x (x = 0.0, 0.25, 0.50, 0.75, 1.0). Table 3 indicates that the largest value of elastic constants related to hexagonal CdSe occurs when we increase Te concentration. Thus, the strongest material from a mechanical viewpoint is the hexagonal CdSe, when shifting from hexagonal CdSe to hexagonal CdTe. Moreover, Table 3 shows that the hexagonal CdSe has the largest longitudinal elastic wave velocity, transverse elastic, average wave velocities and Debye temperature for all changes of x (x = 0.0, 0.25, 0.50, 0.75, 1.0) within LDA exchange-correlation. Our calculations (see Table 3) show that C_{55} has the smallest changes with increasing Te concentration.

In the process of finding linear/non-linear relationships and bowing parameter trends, we fitted the evaluated elastic constants of hexagonal ternary $CdSe_{1-x}Te_x$ alloys in LDA potential with a polynomial of degree 2 for all interested of changes of x (x = 0, 0.25, 0.5, 0.75, 1). The following equations show that C_{11} (C_{55}) has the biggest (smallest) bowing parameter from linearity, thus suggesting the non-linear relation between the elastic constants and Te concentration.

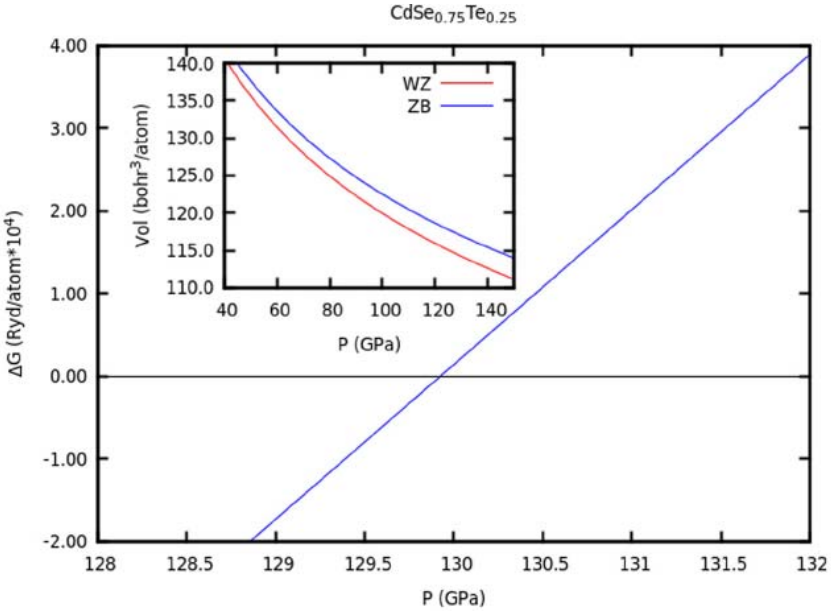

Fig. 2d. Difference of Gibbs free energy as function of pressure for two phases of $CdSe_{0.75}Te_{0.25}$ compound within LDA. The inset: Calculation of the volume versus pressure for two phases.

$$C_{11}(x) = 6.583x^2 - 20.863x + 81.209$$
$$C_{12}(x) = 5.406x^2 - 16.306x + 49.274$$
$$C_{13}(x) = 2.366x^2 - 13.034x + 42.634$$
$$C_{33}(x) = 6.229x^2 - 18.553x + 90.401$$
$$C_{55}(x) = 1.897x^2 - 2.721x + 13.345$$

For elastic stability of hexagonal compounds, three necessary and sufficient conditions [59] (as following) are offered which are evidently satisfied by our calculations.

$$C_{11} > |C_{12}|,\ 2C_{13}^2 < C_{33}(C_{11} + C_{12}),\ C_{55} > 0$$

These three conditions indicate that the hexagonal ternary $CdSe_{1-x}Te_x$ alloys within LDA potential are mechanically stable for all variations of x (x = 0, 0.25, 0.5, 0.75, 1).

Phase transition and stable phase

Our results (Fig. 1(a)–(e)) exhibit that the stable phase for all compositions x of interest (x = 0,0.25,0.5,0.75,1) for bulk ternary $CdSe_{1-x}Te_x$ alloy is zinc-blende (cubic), which is in agreement with the works of Uthanna et al. [14], Mangalhara et al. [15] and Islam et al. [16]. They found that the stable phase for $CdSe_xTe_{1-x}$ $(0 \le x \le 1)$ ternary thin films, independent of composition, is zinc-blende (cubic phase). Additionally, in the new work of Shinde et al. [17] the structure of the $CdSe_{0.6}Te_{0.4}$ thin films was found to be hexagonal.

Using the estimated difference of Gibbs-free-energy ($\Delta G = 0$) at the same pressure grid, it is possible to evaluate the pressure-induced phase transition for two phases of ternary $CdSe_{1-x}Te_x$ alloys.

Our results indicate that DFT + LDA does not foretell a phase transition from cubic to wurtzite for CdTe compound at T = 0 K. Therefore, we can suggest that a phase transition can occur in CdTe compound at a temperature which is not 0 K.

Following Fig. 2(a), our results foresee a possible pressure-induced phase transition from cubic to wurtzite phase for CdSe at a pressure of about 6.1(GPa) using 2D-search of EOS for hexagonal phase. The corresponding volume collapses at the phase-transition boundary are also calculated to be 168.744 ($bohr^3$/atom).

Our results (see Fig. 2(b)) exhibit a possible pressure-induced phase transition from cubic to wurtzite phase for the ternary $CdSe_{0.25}Te_{0.75}$ alloy at pressure of about 11.1 (GPa). The corresponding volume collapses at the phase-transition boundary are also calculated to be 182.646 ($bohr^3$/atom).

Fig. 2(c) indicates a possible pressure-induced phase transition from cubic to wurtzite phase for the ternary $CdSe_{0.5}Te_{0.5}$ alloy at a pressure of about 203.5 (GPa). The corresponding volume collapses at the phase-transition boundary are also calculated to be112.086 ($bohr^3$/atom).

Also, we found that (see Fig. 2(d)) the DFT + LDA calculation predicts a phase transition from cubic to wurtzite for the ternary $CdSe_{0.75}Te_{0.25}$ alloy at pressure of about 129.9 (GPa). The corresponding volume collapses at the phase-transition boundary are also calculated to be 116.969 ($bohr^3$/atom).

Conclusion

A two (one) dimensional search of EOS is used in order to obtain the optimum lattice parameters for $CdSe_{1-x}Te_x$ ternary alloys at different Te compositions (0, 0.25, 0.5, 0.75, 1) for hexagonal (cubic) phase, and to calculate the elastic constants at zero-temperature and zero pressure. The outcomes from our research display that increasing the Te concentration leads to a decrease in the hardness of the structure from the viewpoint of bulk modulus, since the bulk modulus, for both phases of $CdSe_{1-x}Te_x$ within the LDA exchange-correlation, decreases steadily while shifting from CdSe to CdTe. The ZB and WZ phases of $CdSe_{1-x}Te_x$ alloys at various combinations satisfied the mechanical stability conditions at zero K. Elastic constants of ZB and WZ of CdSe have the largest values for all changes of x. This means that, in a mechanical sense, CdSe is the strongest substance in the ternary $CdSe_{1-x}Te_x$ alloys (x = 0.0, 0.25, 0.50, 0.75, 1.0). If we make a comparison between the values of Cauchy pressure and Poisson's ratio, we can say that for both phases of $CdSe_{1-x}Te_x$ ternary alloys (within the LDA exchange-correlation), the ionic bonds are more dominant for all compositions x (x = 0.0, 0.25, 0.50, 0.75, 1.0) of interest. The non-linear relation between the elastic constants and Te concen-

tration can be inferred from our findings. Vickers hardness (Hill's result was utilized) suggests the CdTe as the hardest substance for both phases. The results from our study show that for all compositions x (x = 0.0, 0.25, 0.50, 0.75, 1.0) of interest related to ternary $CdSe_{1-x}Te_x$ alloys the stable phase is zinc-blende. We also noted a possible pressure-induced phase transition from cubic to wurtzite phase for all compositions x (x = 0.0, 0.25, 0.50, 0.75) within LDA exchange-correlation.

Acknowledgments

One of us (M. A.) is indebted to Marco Grilli from Physics Department, La Sapienza University, Rome, Italy for utilizing his computational resources in which part of the calculations is done. Part of this work also has been carried out in the Computational Physics Laboratory, Physics Department, An-Najah N. University.

References

[1] Loizos Z, Spyrellis N, Maurin G, Pottier D. J Electroanal Chem Interfacial Electrochem 1989;269:399.
[2] Muthukumarsamy N, Balasundaraprabhu R, Jayakumar S, Kannan MD. Mater Chem Phys 2007;102:86.
[3] Bailey RE, Strausburg JB, Nie S, Nanosci J. Nanotechnology 2004;4:569.
[4] Velumani S, Mathew X, Sebastian PJ. Solar Energy Mater Solar Cells 2003;76:359.
[5] O'regan B, Gratzel M. Nature 1991;353:737.
[6] Greenham NC, Peng X, Alivisatos AP. Synth Met 1997;84:545.
[7] Gal D, Hodes G, Hariskos D, Braunger D, Schock HW. Appl Phys Lett 1998;73:3135.
[8] Huynh WU, Dittmer JJ, Alivisatos AP. Science 2002;295:2425.
[9] Sharma M, Kumar S, Sharma LM, Sharma TP, Husain M. Curr Appl Phys 2004;4:419.
[10] Sebastianand PJ, Sivaramakrishnan V. J Phys D Appl Phys 1990;23:1114.
[11] Izakason MI, Karasik NYa, Prokator LM, Sakseev DA, Fedorova GA, Yakmimnko IN. InorgMater 1979;15:178.
[12] Bodnar IV, Gurin VS, Molochko AP, Solovei NP, Prokoshin PV, Yumashev KV. Semiconductors 2002;36:298.
[13] Schenk M, Silber C. J Mater Sci Mater Electron 1998;9:295.
[14] Uthanna S, Jayarama P. Reddy. Solid State Commun 1983;45:979.
[15] Mangalhara JP, Thangaraj R, Agnihotri OP. Sol Energy Mater 1989;19:157.
[16] Islam R, Banerjee HD, Rao DR. Thin Solid Films 1995;266:215.
[17] Shinde SK, Dubal DP, Ghodake GS, Fulari VJ. Mater Lett 2014;126:17.
[18] Spagnolo V, Scamarcio G, Lugara M, Righini GC. Superlattices Microstruct 1994;16:51.
[19] Bragas AV, Aku-Leh C, Costantino S, Ingale A, Zhao J, Merlin R. Phys Rev B 2004;69:205306.
[20] Azhniuk YM, Hutych YI, Lopushansky VV, Prots LA, Gomonnai AV, Zahn DRT. Phys Status Solidi C 2009;6:2064.
[21] Smith DL, Pickhardt VY. J Appl Phys 1975;46:2366.
[22] Sanitarov V, Ejovskii U, Kalinkin I, Ansssr IZV. Neorg Mater 1977;13:250.
[23] Irvin J, LaCombe J. J Appl Phys 1974;45:567.
[24] Fayek SA, Elsayed SM. J Phys Chem Solids 2002;63:1.
[25] V.D. Das, in: Proc. SPIE 1523, 326, Conf. On Physics and Technology of Semiconductor Devices and Integrated Circuits, 1922.
[26] Ravichandran D, Xavier FP, Sasikala S, Babu SM. Bull Mater Sci 1996;19:437.
[27] Muthukumarasamy N, Jayakumar S, Kannanand MD, Balasundaraprabhu R. Sol Energy 2009;83:522.
[28] Shinde SK, Ghodake GS, Dubal DP, Lohar GM, Lee DS, Fulari VJ. Ceram Int 2014;40:11519.
[29] Reshak AH, Jamal M. J Alloys Compd 2013;555:362.
[30] Schwarz K, Blaha P, Madsen GKH. Comp Phys Commun 2002;147:71.
[31] Hohenberg P, Kohn W. Phys Rev B 1964;136:864.
[32] Perdew JP, Zunger A. Phys Rev B 1981;23:5048.
[33] Saib S, Benyettou S, Bouarissa N, Ferahtia S. Phys Scr 2015;90:035702.
[34] Perdew JP, Burke K, Ernzerhof M. Phys. Rev. Lett. 1996;77:3865.
[35] Deligoz E, Colakoglu K, Ciftci Y. Phys B 2006;373:124.
[36] Hannachi L, Bouarissa N. Phys B 2009;404:3650.
[37] Benyettou S, Saib S, Bouarissa N. Chem Phys 2015;457:147.
[38] Jamal M, Abu-Jafar MS, Reshak AH. J Alloys Compd 2016;667:151.
[39] 2DRoptimize package is provided by M. Jamal as part of the commercial code WIEN2K, http://www.wien2k.at/ (2014).
[40] gibbs program is provided by M. Jamal as part of the commercial code WIEN2K, http://www.wien2k.at/ (2014).
[41] IRelast package is provided by M. Jamal as part of the commercial code WIEN2K, http://www.wien2k.at/(2014).
[42] P. Blaha, K. Schwarz, G.K.H. Madsen, D. Kvasnika, J. Luitz, WIEN2k, Technical Universität Wien, Austria, 2001, ISBN 3-9501031-1-2.
[43] Jamal M, Kamali Sarvestani N, Yazdani A, Reshak AH. RSC Adv 2014;4:57903.
[44] Jamal M, Jalali Asadabadi S, Ahmad Iftikhar, Aliabad HARahnamaye. ComputMaterSci 2014;95:592.
[45] Heyd J, Peralta JE, Scuseria GE, Martin RL. J Chem Phys 2005;123:174101.
[46] Huang M-Z, Ching WY. Phys Rev B 1993;47:9449.
[47] Mangalhara JP, Thangaraj R, Agnihotrii OP. Solar Energy Mater 1989;19:157.
[48] Madelung O, Schulz M, Weiss H, editors. Landolt-Borstein: Numurical Data and Functional Relationships in Science and Technology, vol. 17. Berlin: Springer; 1982.
[49] Hosseini SM. Phys B 2008;403:1907.
[50] Reshak AH, Kityk IV, Khenata R, Auluck S. J Alloys Compd 2011;509:6737.
[51] R.W.G. Wyckoff (Ed.). Crystal Structures, vol. 1, John Wiley & Sons, Inc., New York, 1963.
[52] McSkimin HJ, Thomas DG. J Appl Phys 1962;33:56.
[53] Madelung O. Semiconductors Data Handbook. Berlin: Springer; 2004. p. 815–35.
[54] Yildirim A, Koc H, Deligoz E. Chin Phys B 2012;21:037101.
[55] Chen XQ, Niu H, Li D, Li Y. Intermetallics 2011;19:1275.
[56] Tian Y, Xu B, Zhao Z. Int J Refract Metal Hardard Mater 2012;33:93.
[57] Born M, Huang K. Dynamical Theory of Crystal Lattices. Oxford: Clarendon; 1954.
[58] Alers GA, Neighbours JR. J Appl Phys 1957;28:1514.
[59] Mouhat Félix, Coudert François-Xavier. Phys Rev B 2014;90:224104.